

Glass forming ability and crystallization of CuTi intermetallic alloy by molecular dynamics simulation

S. SENTURK DALGIC*, M. CELTEK^a

University of Trakya, Science Faculty, Department of Physics, 22030 Edirne, Turkey

^a*University of Trakya, Education Faculty, 22030 Edirne, Turkey*

In this work, we have used molecular dynamics (MD) to obtain an atomistic description of the melting, glass formation and crystallization process in CuTi alloy. We present the tight-binding (TB) many body potentials for the CuTi system which were constructed so as to reproduce a number of properties of the B11 CuTi compound (tetragonal structure). It has been shown that these potentials ensure the stability of the CuTi crystal structure against alternate structures and closely reproduce the melting temperature of CuTi. We have also considered several cooling rates to investigate its effect on the glass transition and crystallization temperatures. The pair distribution functions (PDF), Wendt–Abraham (WA) parameters and the changes of volume were calculated to determine glass transition temperature and crystal formation of CuTi alloy.

(Received June 2, 2011; accepted November 23, 2011)

Keywords: Glass, CuTi alloy, Molecular dynamics simulation

1. Introduction

Metallic glass was first prepared by rapid quenching from the melt for Au₈₀Si₂₀ in 1960 [1]. Since then much effort has been devoted to the development of bulk metallic glasses (BMGs) for both fundamental scientific research and industrial applications. The successful synthesis of bulk metallic glasses during the late 1980s has stimulated great enthusiasm in the study of metallic materials. The mostly binary metallic glass forming alloys must be rapidly quenched with rates up to 10⁶ K/s for vitrification. However, the high cooling rate prevents the practical applications of the amorphization technique.

More recently, the new generation of BMGs have been developed with much lower critical cooling rates of 100K/s to 1K/s [2, 3]. Since 1990s, many innovations have been achieved concerning the understanding of physical, chemical, and mechanical properties of BMGs. Bulk metallic glasses are promising materials because of their superior properties and relatively lower materials cost. The understanding of structure and thermal stability of BMGs is of great importance from both the fundamental and practical viewpoints. BMG formation and glass forming ability (GFA) in binary Cu-Ti alloys have been studied by some researchers [4, 5]. The atomic structures of the binary BMGs of Cu_xTi_{1-x} alloys have also been analyzed experimentally by Sakata et.al. [6], Gržeta et.al [7], Rodmacq et. al. [8], Ivison et. al. [9] and Yamada et. al.[10]. The molecular dynamics (MD) simulations for Cu_xTi_{1-x} systems was performed with Finnis-Sinclair (FS) [11], the modified embedded-atom method (MEAM) [12] and the embedded-atom method (EAM) potentials [13, 14] in order to determine their different physical properties. According to our knowledge, no structural calculations have been performed on Cu-Ti alloys using Tight Binding (TB) many body potentials coupled with MD simulations.

The purpose of the present work is the test of transferability of TB potential for the Cu-Ti binary system which is based on previously developed for pure Cu and Ti by Cleri and Rosato [15]. In our previous studies, it has been shown that the TB potentials were successful in determining the glass forming ability (GFA) and structural properties of ternary Cu₅₀Ti₂₅Zr₂₅ [16] and Cu_{55-x}Zr₄₅Ag_x (x=0,10,20) [17] alloys.

In this work, we present simulated results of the BMG-forming Cu₅₀Ti₅₀ binary alloy. In order to investigate the GFA of the Cu₅₀Ti₅₀ binary alloy in an atomic level, the TB potential of binary Cu,Ti system was newly developed. This potential yields the liquid to glass and crystallization transition for binary Cu₅₀Ti₅₀ alloy, in reasonable agreement with experimental information.

2. Method

As a first step in MD simulations, it is necessary to describe the atomic motions. In this study we have used a quantum mechanics based TB potential [15] to describe the atomic motions and to explain the structural properties. In TB model, the energy of a single atom can be divided in to two parts as attractive and repulsive ones. The attractive part can be given as,

$$E_B^i = - \left\{ \sum_j \xi_{\alpha\beta}^2 \exp \left[- 2q_{\alpha\beta} \left(\frac{r_{ij}}{r_0^{\alpha\beta}} - 1 \right) \right] \right\}^{1/2} \quad (1)$$

where r_{ij} represents the distance between atoms i and j . The α and β variables represent species of different lattice of unlike neighboring atoms, $r_0^{\alpha\beta}$ is the distance between first-neighbours of species α and β , $\xi_{\alpha\beta}$ is an effective

hopping integral and $q_{\alpha\beta}$ describes its dependence on the relative inter atomic distance..

The repulsive interaction term is normally assumed to be pair-wise, and described by a sum of Born-Mayer ion-ion repulsions:

$$E_R^i = \sum_j A_{\alpha\beta} \exp \left[-p_{\alpha\beta} \left(\frac{r_{ij}}{r_0^{\alpha\beta}} - 1 \right) \right] \quad (2)$$

where $A_{\alpha\beta}$ is dependent on the experimental values of the lattice parameter. The parameter $p_{\alpha\beta}$ is related to the compressibility of the bulk metal. For the hetero-interactions, an arithmetic mean was taken for the parameters related to the distance, $p_{\alpha\beta}$, $q_{\alpha\beta}$ and $r_0^{\alpha\beta}$, while a geometric mean was taken for parameters related to the strength, $A_{\alpha\beta}$ and $\xi_{\alpha\beta}$. The total energy of the system can be described as

$$E_C = \sum_i (E_R^i + E_B^i) \quad (3)$$

In the present study, the many body type TB potential was adopted to simulate of $\text{Cu}_{50}\text{Ti}_{50}$ alloy. In our simulations, we have used the simulation code of DL_POLY [18].

The MD simulations are performed on a cubic box with 1372 atoms subjected to the periodic boundary conditions along all the three directions. The model system that represents the γ -phase CuTi compound has a tetragonal B11 structure and contains 1372 atoms, equally divided between Cu (686 atoms) and Ti (686 atoms). Based on constant temperature and constant pressure NPT ensemble with the Berendsen thermostat has been used to control the temperature and pressure. The pressure was kept at 0 Pa.. The Newtonian equations of motion are integrated using the Leapfrog Verlet algorithm with a time step of 2 fs, this value sufficiently small to reduce the fluctuations of the total energy.

The stable structure at 0K is obtained through the initial configurations annealed fully at $T=300\text{K}$ and then cooled to $T=0\text{K}$ at a cooling rate of 0.25 K/ps. A series of temperature increases from 0 K to 1600K with an increment of $\Delta T=50\text{K}$ for TB potential in the simulation of the melting process. Before starting the cooling process of the system, we equilibrated the liquid system at 1600K using constant temperature and constant volume (NVT) ensemble with 200000 steps. Then, cooled down to 300K with six different cooling rates of 10 K/ps, 5 K/ps, 0.5 K/ps, 0.1 K/ps, 0.05 K/ps and 0.01K/ps to testing the effect of cooling rate on glass transition temperature T_g and crystallization temperature T_x .

The pair distribution function PDF has been widely used to describe the structural variations between liquid, amorphous and crystalline structures, and given as

$$g(r) = \frac{V}{N^2} \left\langle \sum_i \sum_{i \neq j} \delta(r - r_{ij}) \right\rangle \quad (4)$$

where N is the number of atoms in the simulation box. The $g(r)$ shows the probability of finding another atom at a distance r from an origin atom.

3. Results and discussion

The MD simulations have been performed with TB potential at 0.5 K/ps heating rate and six different cooling rates of 10 K/ps, 5 K/ps, 0.5 K/ps, 0.1 K/ps, 0.05 K/ps and 0.01 K/ps,. Some macroscopic description of the $\text{Cu}_{50}\text{Ti}_{50}$ system, such as volume, structure, glass and crystallization temperatures are obtained from the NPT MD cooling runs. The input potential parameters for Cu-Cu, Cu-Ti and Ti-Ti pairs are listed in Table 1.

Table 1. TB potential parameters for CuTi system.

	$A_{\alpha\beta}$ (eV)	$\xi_{\alpha\beta}$ (eV)	$p_{\alpha\beta}$	$q_{\alpha\beta}$	$r_0^{\alpha\beta}$ (Å)
Cu-Cu	0.08550	1.2240	10.960	2.278	2.556
Cu-Ti	0.11395	1.4849	9.7900	2.334	2.725
Ti-Ti	0.15190	1.8112	8.6200	2.390	2.890

Lattice parameters for all four phases (B11, B2, L1₀ and B19) of CuTi alloy have been calculated with many body type TB potential, as given in Table 2. The obtained values for lattice parameters, cohesive energy E_c and atomic volume for B11 γ -CuTi tetragonal structure are compared with the experimental data [19-23] and results those obtained by *ab initio* method [24] in Table 2. It has been found that the MD simulated results are in good agreement with experimental lattice parameters and atomic volume values. As a result of this, our obtained values are more compatible with experimental data than those obtained from the MEAM potential [12]. In the same way, the lattice parameters obtained for the other L1₀ (space group P4/mmm #123), B19 (space group Pmma #51) and B2 (space group Pm $\bar{3}$ m #221) CuTi compounds are in good agreement with results obtained by *ab initio* method [24]. In this work, we focus on MD study of stable B11 γ -CuTi tetragonal structure.

We have considered six cooling rates to investigate its effect on the glass transition temperature T_g and crystallization temperature T_x . Fig. 1. shows the temperature dependence of the volume of $\text{Cu}_{50}\text{Ti}_{50}$ binary alloy at the heating rate of $\gamma=0.5$ K/ps and at the cooling rates of $\gamma=10$ K/ps, $\gamma=5$ K/ps, $\gamma=0.5$ K/ps, $\gamma=0.1$ K/ps, $\gamma=0.05$ K/ps. and $\gamma=0.01$ K/ps. In order to obtain the melting temperature T_m and liquidus temperature T_l , we have used $\Delta T=10\text{K}$ increment in the temperature range from 950K to 1300K. The phase transition in $\text{Cu}_{50}\text{Ti}_{50}$ binary alloy has been defined by using two concepts: i) a sudden increase in volume corresponds to the temperature range of 1180K–1190K during heating process is due to the melting of the $\text{Cu}_{50}\text{Ti}_{50}$ alloy. ii) the change of the total pair distribution functions (PDF) from crystal form to liquid form given in Fig. 2.

Table 2. Some physical properties for four optimized structures of CuTi, together with experimental data and result from *ab initio* calculations, lattice constants a , b , and c are expressed in \AA , the cohesive energy E_c in eV/atom and the atomic volume Ω in $\text{\AA}^3/\text{atom}$.

Compound	Structure type	Pearson symbol	Exp.	<i>Ab initio</i>	MEAM	TB
CuTi	γ CuTi (B11)	tP4	$E_c=4.2814^a$	$E_c=4.2258^e$		$E_c=4.2115$
			$a=3.1070^b$	$a=3.1256^e$	$a=3.0850^f$	$a=3.1075$
			$a=3.1080^c$	$a=3.1256^e$	$a=3.0850^f$	$a=3.1075$
			$c=5.9190^b$	$c=5.9152^e$	$c=6.3700^f$	$c=5.8860$
			$c=5.8870^c$			$c=5.8860$
			$\Omega=14.217^d$			$\Omega=14.209$
CuTi	AuCu (L1 ₀)	tP2		$a=3.8202^e$		$a=3.8159$
	CsCl (B2)	cP2		$c=3.9079^e$		$c=3.9040$
	AuCd (B19)	oP4		$a=3.0804^e$		$a=3.0569$
				$a=4.4469^e$		$a=4.4459$
				$b=2.6823^e$		$b=2.6817$
				$c=4.7911^e$		$c=4.7901$

^aRef [19], ^bRef [20], ^cRef [21, 22], ^dRef [23], ^eRef [24], ^fRef [12]

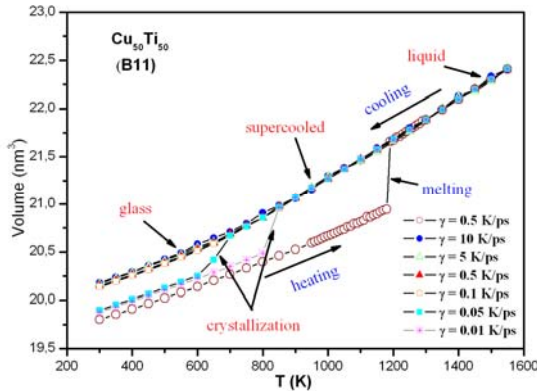


Fig. 1. The temperature dependence of volume of $\text{Cu}_{50}\text{Ti}_{50}$ binary alloy at heating and cooling process.

The calculated liquidus temperature $T_l=1190\pm 5\text{K}$ and melting temperature $T_m=1180\pm 5\text{K}$ are in good agreement with the experimental temperatures, $T_l=1248\text{K}$

[4] and $T_l=1218\text{K}$, $T_m=1171\text{K}$ [5]. The volume curves above melting temperature almost overlap between the different cooling rates. This shows that the atoms can move rapidly enough based on the temperature change. The volume drops linearly based on the decreasing temperature. The volume changes continuously during at the four cooling rates, $\gamma=10\text{ K/ps}$, $\gamma=5\text{ K/ps}$, $\gamma=0.5\text{ K/ps}$ and $\gamma=0.1\text{ K/ps}$.

However the temperature decreasing below 700K, the volume changes show difference for the different cooling rates. This indicates the formation of a metallic glass. Different cooling rate leads to different crystallization

temperature, the larger the cooling rate, the lower the crystallization temperature.

When the slower cooling rates of 0.05 K/ps and 0.01 K/ps are used in the simulation, it is observed that the volume changes have big breaks about 700K and 850K with decreasing temperature, respectively. This break shows that liquid to crystallization transition occurs.

The way we follow to predict the melting temperature from the total pair distribution function (PDF) to be correct is observed in Fig. 2 as plotted at the selected temperatures; 1180K and 1190K for $\text{Cu}_{50}\text{Ti}_{50}$ binary alloy. As shown in Fig. 2, the total pair distribution function shows a crystal structure as the sample is heated at 1180K temperature. However, above melting at 1190K the emergence of broad peaks shows that the structure has melted.

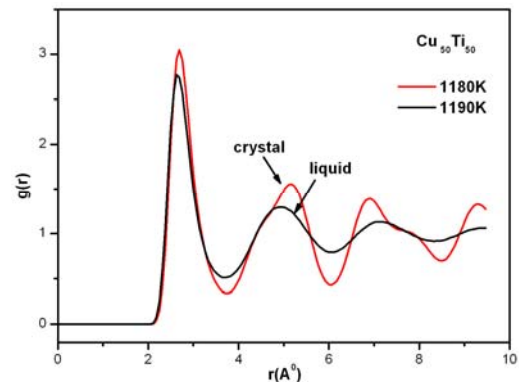


Fig. 2. The total pair distribution functions at the near melting point of $\text{Cu}_{50}\text{Ti}_{50}$ binary alloys during heating process.

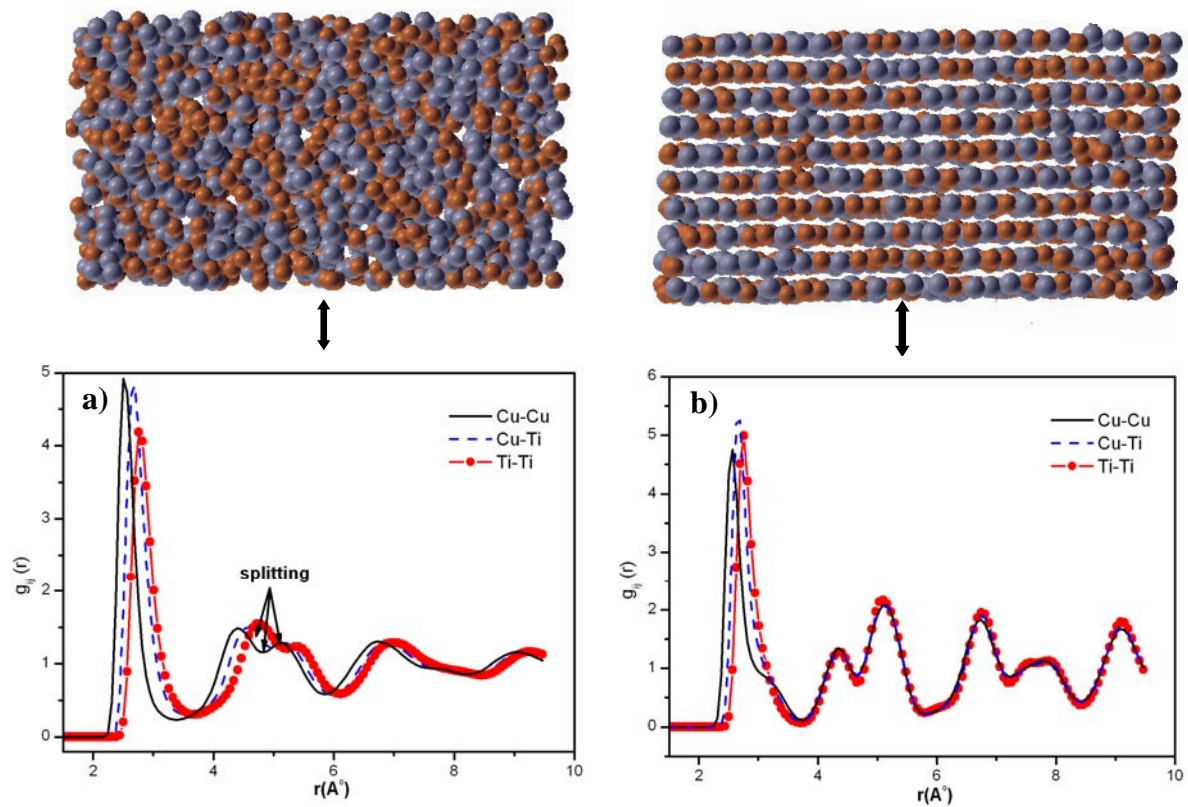


Fig. 3. The projections of the atomic positions on the y-z plane and partial pair distribution function of $\text{Cu}_{50}\text{Ti}_{50}$ binary alloy at 300K for two different cooling rates; a) 0.5K/ps cooling rate and b) 0.05K/ps cooling rate. The orange and gray balls represent Cu and Ti atoms, respectively.

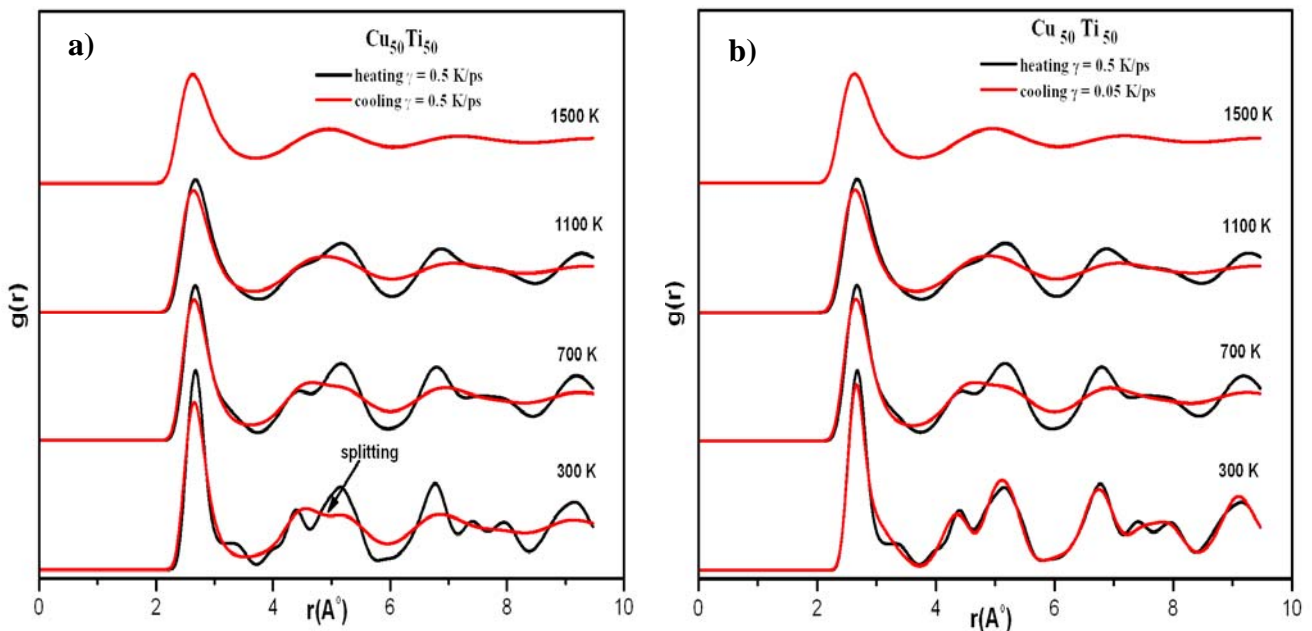


Fig. 4. The total PDF of $\text{Cu}_{50}\text{Ti}_{50}$ at various temperatures for the heating (black lines) and cooling processes (red lines) at a) $\gamma = 0.5$ K/ps cooling rate and b) $\gamma = 0.05$ K/ps cooling rate.

Fig. 3 shows the two-dimensional cross-sectional projections of the structures and the simulated partial pair distribution functions (PPDFs) $g_{ij}(r)$ for Cu-Cu, Cu-Ti, and

Ti-Ti pairs obtained with two different cooling rates, 0.5 K/ps and 0.05 K/ps. As shown in our MD calculations during the cooling processes with cooling rate 0.5 K/ps,

the second peak of all atom pairs, Cu-Cu, Cu-Ti and Ti-Ti splitting show up the temperature at 300K. We have also examined the PPDFs for all pairs at the four different cooling rates of 10 K/ps, 5 K/ps, 0.5 K/ps and 0.1 K/ps used in this study and similar PPDFs have been obtained for all pairs. When cooling down to 300K at the slow cooling rate of 0.05 K/ps, the partial pair distribution functions $g_{ij}(r)$ for all atom pairs are seen with crystal structure. This behavior of PPDFs was observed in the slow cooling rate of 0.01K/ps.

We examine the structural properties of the $\text{Cu}_{50}\text{Ti}_{50}$ binary alloy in the liquid, supercooled liquid, amorphous and crystal states in Fig. 4 by analyzing the pair distribution function (PDF) during heating process and cooling process at two different cooling rates. As shown in Fig. 4 (a). and Fig. 4 (b), two curves of PDF during heating and cooling processes overlap at the same temperature (at $T=1500\text{K}$) as indicating an equilibrium liquid state. When the system is cooled to 1100K with both the cooling rates of 0.5 K/ps and 0.05 K/ps, we still

observe the structure of liquid, in fact a supercooled region, while system is crystalline state during heating process at same temperature. Liquid in the region between melting temperature and noticeable bend is so-called supercooled liquid.

Cooling to 300K using 0.5 K/ps cooling rate, it is seen a splitting at second peak of $g(r)$ which known as characteristic behavior of metallic glasses. On the other hand, when cooling down to 300K at the slow cooling rate of 0.05K/ps, the peaks for heating and cooling processes almost overlap with B11 tetragonal structure.

The structure factors $S(q)$ obtained directly from the experimental data are perhaps the best curves for comparison between experiment and simulation. As a further test, we determined the total structure factor of $\text{Cu}_{50}\text{Ti}_{50}$ alloy in the glassy state of 400 K on the basis of this model. The simulation result is shown in Fig. 5, which also includes the experimental data of Grzeta et al. from an x-ray diffraction [7].

Table 3. The Glass forming ability (GFA) parameters of $\text{Cu}_{50}\text{Ti}_{50}$ binary alloy obtained from a heating rate of 0.5 K/ps and six different cooling rates.

Composition	Process	γ^{MD} (K/ps)	T_g (K)		T_m (K)		T_x (K)		T_l (K)		$T_{rg} = T_g/T_m$		
			MD	Exp.	MD	Exp.	MD	Exp.	MD	Exp.	MD	Exp.	
$\text{Cu}_{50}\text{Ti}_{50}$	heating	0.5			1180±5	1171 ^a			1190±5	1218 ^a			
	cooling	10	680	658 ^a			-				1248 ^b		
		5	674				-				0.576	0.562 ^a	
		0.5	630				-				0.571		
		0.1	615				-				0.534		
		0.05	-					700	682 ^a			0.521	
0.01	-					850					-		

^aRef [5], ^bRef [4]

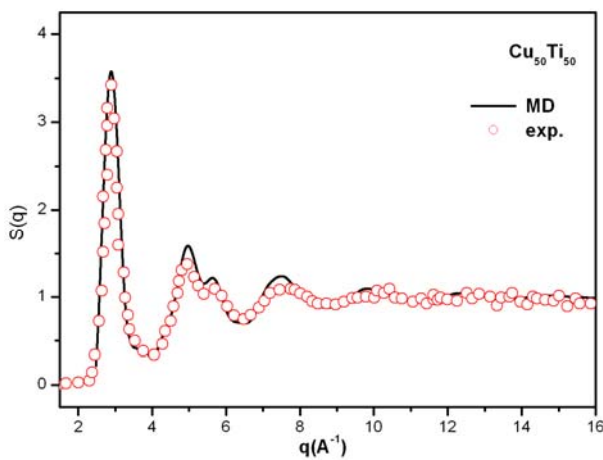


Fig. 5. (Color online) Total structure factor of experimental [7] and simulated amorphous $\text{Cu}_{50}\text{Ti}_{50}$ at 400K.

As shown in Fig. 5, a splitting, which is suitable with each other, is seen in the second maximum peaks of the structure factors obtained from experimental and simulation. This splitting is known as the main characteristic behavior of metallic glasses. The good agreement between simulation and experimental results are found. It indicates that our microscopic model is quite suitable to describe the atomic interactions of the $\text{Cu}_{50}\text{Ti}_{50}$ binary alloy system.

It has been shown in Table 3 that the simulated melting temperature of TB potential is about 1180K during the heating rate of 0.5 K/ps that is 9K higher than the reported experimental value given in Ref [5]. The calculated other values, i.e. the reduced glass-transition temperature T_{rg} , glass transition temperature T_g , liquidus temperature T_l , are compatible with experimental data.

In this study Wendt-Abraham (WA) parameter ($R^{\text{WA}} = g_{\text{min}}/g_{\text{max}}$) is used to obtain glass transition temperature T_g . Here g_{min} is first minimum value and g_{max} first maximum value of PDF curve. The Wendt-Abraham

parameter emphasizes the local character of $g(r)$ permitting a direct comparison between structures and leading to a better estimation of T_g . We have considered different cooling rates to investigate its effect on the glass transition temperature T_g . Figure 6. gives the temperature dependence of WA parameters at the six different cooling rates. The model system shows a glass formation at temperatures 680K, 674K, 630K and 615K at the cooling rates of 10 K/ps, 5 K/ps, 0.5 K/ps and 0.1 K/ps, respectively. WA parameter curves versus temperature obtained with the four cooling rates are shown in detail for the temperature range of 300K-800K at top of Figure6. As shown at top of Fig. 6, the cooling rates of 10 K/ps, 5 K/ps, 0.5 K/ps and 0.1 K/ps leads to a slightly different slope value. The $\text{Cu}_{50}\text{Ti}_{50}$ BMG alloy shows a glass formation at the fast cooling rates, while the slower cooling rate of 0.05 K/ps and 0.01 K/ps leads to crystallization about 700K and 850K, respectively.

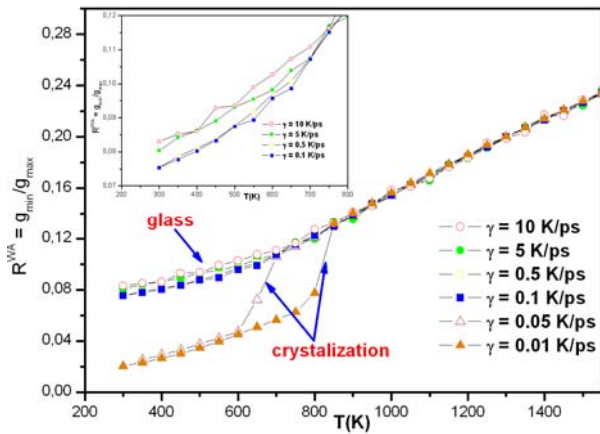


Fig. 6. WA parameters versus temperature for $\text{Cu}_{50}\text{Ti}_{50}$ binary alloy obtained using TB potential.

Fig 7. shows that g_{\min}/g_{\max} is fitted to linear function to estimate the glass temperature at the cooling rate of 0.5 K/ps. This procedure was also performed for other cooling rates of 10 K/ps, 5 K/ps, 0.5 K/ps and 0.1 K/ps. Reduced glass-transition temperature (T_{rg}) can thus obtained by simply dividing glass transition temperature (T_g) by liquidus temperature (T_l) or melting temperature (T_m) as $T_{rg}=T_g/T_l$ or $T_{rg}=T_g/T_m$. Table 3. lists glass transition temperature (T_g), liquidus temperature (T_l), melting temperature (T_m), crystallization temperature (T_x) and reduced glass-transition temperature T_{rg} obtained using many body type TB interatomic potential comparing with the experimental values given in Ref. [5].

The reduced glass-transition temperature (T_{rg}) values obtained with cooling rates of 10 K/ps, 5 K/ps, 0.5 K/ps and 0.1 K/ps have been calculated as 0.576, 0.571, 0.530 and 0.515, respectively. The calculated range of value is also compatible with experimental value 0.562 [5].

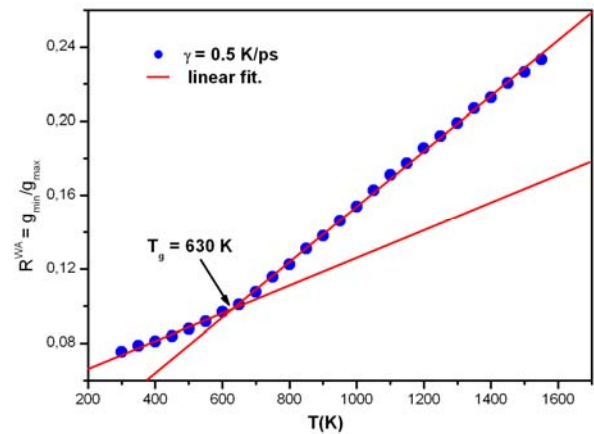


Fig. 7. Temperature dependence of g_{\min}/g_{\max} values fitted to a linear function to estimate the glass temperature T_g at the cooling rate of $\gamma = 0.5$ K/ps.

4. Conclusions

The present study reports the results from MD modeling of the binary $\text{Cu}_{50}\text{Ti}_{50}$ alloy with NPT and NVT molecular dynamics simulation. The many body type TB interatomic potential is used to investigate the GFA ability of this binary system. There is a good agreement between the MD simulated and experimental GFA parameters such as T_g , T_l , T_{rg} and T_x values. It has been noted that the glass transition temperature depends on the cooling rate; the larger cooling rates give the higher glass transition temperature.

The many body type TB potential produces crystal structure during the cooling rates of 0.05 K/ps and 0.01 K/ps, while it produces amorphous structure for cooling rates of 10 K/ps, 5 K/ps, 0.5 K/ps and 0.1 K/ps.

Pair distribution functions (PDF) and total structure factor have calculated to analyze the local structure of B11 (tetragonal structure) $\text{Cu}_{50}\text{Ti}_{50}$ metallic glasses. When the system is cooled with different larger cooling rates, the splitting of the second peak of $g(r)$ appears in the glass state. In the same way, when the system is cooled with slow cooling rates, pair distribution functions and total structure appear in crystal structure.

In summary, TB potentials for the $\text{Cu}_{50}\text{Ti}_{50}$ binary alloy system is now available to show the glass transition temperature and crystallization of this alloy.

References

- [1] W. Klement, R. H. Willens, P. Duwez, Nature **187**, 869 (1960).
- [2] A. Peker, W. L. Johnson, Appl. Phys. Lett. **63**, 2342 (1993).
- [3] W. L. Johnson, MRS Bull. **24**, 42 (1999).
- [4] H. Men, S. J. Pang, T. Zhang, Mater. Sci. Eng. A **408**, 326 (2005).
- [5] T. Lin, J. Jiang, X.-F. Bian, Y. Dong, Trans. Nonferrous Met. Soc. China **16**, 604 (2006).

- [6] M. Sakata, N. Cowlam, H. A. Davies, *J. Phys. F: Metal Phys.* **9**, 12 (1979).
- [7] B. Gržeta, K. Dini, N. Cowlam, H. A. Davies, *J. Phys. F: Met. Phys.* **15**, 2069 (1985).
- [8] B. Rodmacq, P. Mangin, A. Chamberod, *J. Phys. F: Met. Phys.* **15**, 2259 (1985).
- [9] P. K. Ivison, I. Soletta, N. Cowlam, G. Cocco, S. Enzo, L. Battezzati, *J. Phys.: Condens. Matter* **4**, 163 (1992).
- [10] M. Yamada, N. Matsui, N. Kamilya, K. Miyazaki, K. Tanaka, *Materials Transactions, JIM* **35**, 1 (1994).
- [11] D. T. Kulp, G. J. Ackland, M. Šob, V. Vitek, T. Egami, *Modelling Simul. Mater. Sci. Eng.* **1**, 315 (1993).
- [12] Y.-M. Kim, B.-J. Lee, *Materials Science and Engineering A* **449**, 733 (2007).
- [13] M. J. Sabochick, N. Q. Lam, *Phys. Rev. B.* **43**, 5243 (1991).
- [14] M. Neudecker, S. G. Mayr, *Acta Materialia* **57**, 1437 (2009).
- [15] F. Cleri, V. Rosato *Phys. Rev. B* **48**, 22 (1993).
- [16] S. S. Dalgic, M. Celtek, *EPJ Web of Conferences* **15**, 03008 (2011).
- [17] S. S. Dalgic, M. Celtek, *EPJ Web of Conferences* **15**, 03009 (2011).
- [18] DL_POLY: a molecular dynamics simulation package written by W. Smith, T.R. Forester and I.T. Todorov has been obtained from the website http://www.ccp5.ac.uk/DL_POLY
- [19] O. J. Kleppa, S. Watanabe, *Metal. Trans. B* **13**, 391, (1982).
- [20] V. N. Eremenko, Y. I. Buyanov, S. B. Prima, *Sov Powder Metall. Met. Ceram* **5**, 494 (1966)
- [21] N. Karlsson, *J. Instr. Met.* **79**, 391 (1951).
- [22] Y. C. Kim, D. H. Bae, W. T. Kim, D. H. Kim, *Journal of Non-Crystalline Solids* **325**, 242 (2003).
- [23] A. J. C. Wilson, *International Union of Crystallography, Utrecht* **15**, 69 (1951).
- [24] G. Ghosh, *Acta Mater.* **55**, 3347 (2007).

*Corresponding author: serapd@trakya.edu.tr